Formation Sensing and Control Technologies for a Separated Spacecraft Interferometer[1]

Andrew Robertson[2], Tobé Corazzini[3] and Jonathan P. How[4]
Stanford University

Abstract

This paper describes spacecraft formation control and sensing research with application to a Separated Spacecraft Interferometer. A multi-layer control design that achieves very accurate alignment between spacecraft is described. Sensing for this control architecture is based on a global real-time relative position and orientation estimator that uses Carrier Differential-phase GPS measurements. A local optical sensor is used as well. The experiments are performed on a fully functional indoor GPS environment using three prototype spacecraft on a granite table. Work continues on extending the control to a formation of three active vehicles and on extending the sensing system to a *self-constellation*.

1 Introduction

Formation flying of multiple spacecraft is an enabling technology for many future space science missions including enhanced stellar optical interferometers and *virtual platforms* for space science in low Earth orbit. This paper describes research on the development of an indoor multi-vehicle, GPS-equipped testbed to demonstrate various navigation and control issues associated with this class of missions. The objective of this work is to investigate the sensing, initialization, and control of a multiple spacecraft system such as the New Millennium Interferometer (NMI) [1]. Our *systems approach* of analyzing and testing on this testbed complements on-going research at NASA JPL [2].

To fly spacecraft in a precise formation, it is necessary to develop a very accurate real-time sensor for the formation position and attitude. The Carrier Differential-phase techniques of the Global Positioning System (CDGPS) offer a very promising method for sensing the relative state (position and attitude) of these vehicles [3]. CDGPS techniques have already been demonstrated on-orbit for the attitude determination of a spacecraft [4] and were originally proposed as a sensor for the NMI in Ref. [5]. Zimmerman [6] used these same CDGPS techniques to provide centimeter-level precision for relative positioning between two vehicles. This work was done using an indoor setup with pseudolites [7] to generate the GPS signal. This represents an intermediate step towards placing the pseudolite transmitters on-board the vehicles themselves, thereby enabling GPS sensing to be used in *self-constellation* mode when the NAVSTAR constellation is not visible.

The NMI mission requires a very tight formation of three spacecraft that will necessitate the development of many different sensing and control technologies. Two of the spacecraft will act as collectors that focus the light of a distant star onto the third combiner spacecraft that forms the interference pattern [1]. To form the interference pattern, the optical path between the spacecraft must be controlled to within a fraction of a wavelength of light. A layered control approach has been proposed to achieve this high degree of accuracy. The current mission plan would use CDGPS-like sensors as a coarse sensing layer to measure the spacecraft relative position to within 4 cm and relative attitude to within 6 arcsec so that the more accurate optical metrology systems can be aligned.

This paper focuses on recent developments at Stanford to provide a two-dimensional, three vehicle formation flying testbed (FFTB) that can be used to investigate many of the sensing and control issues associated with a separated spacecraft interferometer. The current work extends previous research [6, 8, 9] which developed a formation of three active vehicles using GPS sensing to determine the relative position and attitude. Results to date have shown that a CDGPS based relative sensing system achieves accuracies better than 2 cm and 0.5° on a real formation of vehicles.

Research topics include:

1. Formation control: investigation of the key trade-offs associated with various estimation, communication, and control architectures on the FFTB.
2. Formation sensing: enhancing the relative navigation by developing reliable acquisition procedures and extending the CDGPS-based sensing to a self-constellation system.

The results presented here represent one step in the process of identifying issues and developing enabling technologies for the separated spacecraft interferometer. CDGPS continues to show promise as an accurate global sensor; the improvements presented here allow real-time control with feedback on the CDGPS relative position and velocity estimates. The systems approach to designing the multi-layer alignment control will be continued as three active vehicles

[1]Included in the Interferometry Modeling and Control Session of the American Control Conference, Philadelphia, PA, June 24-26, 1998
[2]Ph.D. candidate in the Dept. of Aeronautics and Astronautics, *adr@sun-valley.stanford.edu*
[3]Ph.D. candidate in the Dept. of Aeronautics and Astronautics, *tobe@sun-valley.stanford.edu*
[4]Assistant Professor in the Dept. of Aeronautics and Astronautics, *howjo@sun-valley.stanford.edu*

Figure 1: Formation Flying Testbed.

are coordinated to act together as a single instrument system.

2 Formation Flying Testbed

To investigate the guidance, navigation, and control issues associated with the precision formation flying NMI mission, a formation flying testbed has been created in the Stanford Aerospace Robotics Laboratory. The testbed consists of 3 active free-flying vehicles that move on a 12 ft × 9 ft granite table top (see Figure 1). These air cushion vehicles simulate the drag-free zero-g dynamics of a spacecraft formation in a horizontal plane. The self-contained vehicles are propelled by compressed air thrusters.

An indoor GPS environment was previously constructed by Zimmerman [10]. This consists of six ceiling mounted pseudolite transmitters broadcasting GPS signals.

Each vehicle has four GPS antennas connected to a single GPS TANS (Quadrex) receiver. There is an overhead vision system mounted above the table that can track each vehicle in real-time. The vision system has an absolute accuracy better than 1 cm for position and 1.5° for attitude for the entire table. This testbed is augmented with a simple laser metrology system to investigate the coarse/fine acquisition process and to measure the overall system performance.

3 Position and Attitude Estimation

Ref. [9] provides a detailed derivation of the equations used to estimate the relative position and attitude of the vehicles using GPS carrier phase measurements. The measured carrier phase at antenna j of vehicle i from pseudolite k is

$$\phi_{ijk} = |S_{ijk}| + c\tau_{vi} + c\tau_{pk} + \lambda K_{ijk} \tag{1}$$

where S_{ijk} is a vector from the phase center of the pseudolite antenna to the phase center on each receive antenna. The terms $c\tau_{vi}$ and $c\tau_{pi}$ represent the portion of the phase incurred by clock errors between the transmitter and the receiver, and are the dominating terms in the measurement equations. These terms are eliminated by differencing over measurements from multiple antennas and vehicles. The antenna location relative to the pseudolite is clearly a function of the vehicle position and attitude, and thus S_{ijk} is a function of the vehicle state X_i.

The intra-vehicle single differences contribute primarily to determination of the attitude of each vehicle. These measurements are obtained by differencing between the master antenna ($j = m$) and each of the slave antennas j of vehicle i for measurement from pseudolite k:

$$\Delta\phi_{ijk} = |S_{imk}| - |S_{ijk}| + \lambda M_{ijk} \tag{2}$$

$\forall k$ and $\forall j \neq m$. The M_{ijk} are the intra-vehicle integers.

The inter-vehicle double differences contribute primarily to the relative position measurements between vehicles. With N pseudolites there are $N-1$ unique double differences between pseudolites k_1 and k_2 ($k_1 \neq k_2$). These differences are calculated to eliminate the remaining effects due to clock errors $c(\tau_{v1} - \tau_{v2})$

$$\begin{aligned} \nabla\Delta\phi_{ijk_1k_2} &= |S_{imk_1}| - |S_{jmk_1}| \\ &- (|S_{imk_2}| - |S_{jmk_2}|) + \lambda N_{ijk_1k_2} \end{aligned} \tag{3}$$

$\forall k_1$, k_2 with $k_1 \neq k_2$. The $N_{ijk_1k_2}$ in Eq. 3 refers to the inter-vehicle integers.

Given the phase measurements for the vehicle formation, the optimal estimate of the formation states $X_i(t)$ can be solved in real-time using nonlinear estimation techniques. It is also necessary to obtain an estimate of the single and double difference integer ambiguities so that these can be subtracted from the phase measurements. For the results presented in this paper the vehicles are started at known locations so that the integers can be solved for directly [11]. Both Refs [8, 9] discuss more sophisticated integer resolution approaches based on the motion and search techniques [12, 13]. These initial results are promising, and work continues on implementing these approaches on the testbed shown in Figure 1.

While these vehicles solve for their absolute states (position and orientation), what is more important for the formation sensing and control are the relative states which can be found by simply subtracting the two absolute state estimates. In general it is expected that this sensing system will provide a more accurate estimate of the relative position between vehicles because many of the most important error sources are predominantly common-mode and their effects are removed by differencing the absolute position estimates.

4 Formation Flying System

A two-vehicle stationkeeping system is used to investigate the advanced GPS-based formation sensing and formation control techniques discussed in this paper. Two GPS-equipped simulated spacecraft are assigned the task of keeping station 1.2 meters apart. One vehicle is kept passive; the other maintains the relative state (position and orientation) using thrusters. In addition, a laser pen mounted on the active vehicle is aimed at a 14 cm wide target on the passive vehicle. The goal of the active vehicle is to keep the laser pen pointed at the center of the target to within a given tolerance. The active vehicle has thrusters for position and attitude control plus a reaction wheel for fine attitude control.

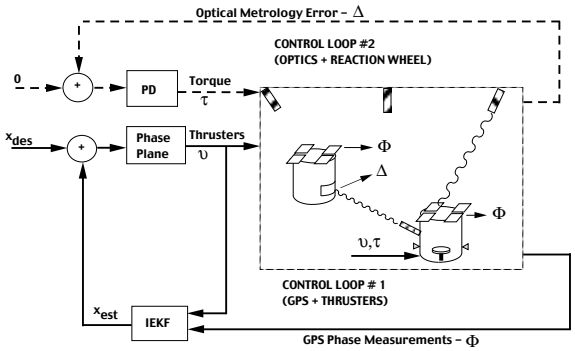

Figure 2: Two-vehicle stationkeeping control strategy.

This two vehicle system is designed to address some of the key challenges faced by a separated spacecraft interferometer. In particular, for this system we need an accurate, but global, relative sensor for coarse stationkeeping control. This outer most layer of the control is designed to keep the laser point on the target. A fine pointing controller can then be used to move the laser point to the center of the target, thereby accurately aligning the two vehicles. These features are similar to the functions of the NMI spacecraft which will have to move to desired locations (e.g. at initialization or during retargeting) and then align with sufficient accuracy that the optical metrology loops can be closed.

For our system, the coarse sensor is an indoor GPS system (as described in Section 2) and the fine sensor is a CCD camera mounted on the passive vehicle. The camera looks down at the target plate. The camera signal is processed and if the laser end-point is on the target, its position is reported. Each of these two sensors generates a signal that is used in a feedback loop to control the active vehicle.

As discussed in the next section, the GPS signals from both robots are processed by an iterated extended Kalman filter to generate a relative state (position and orientation) and relative rate estimate. This estimate is fed into a phase plane controller (Section 6) which uses the thrusters to keep the relative state within a desired error range. When available, the laser position (as determined by the camera) is used in a simple proportional-derivative control which uses the reaction wheel to keep the laser dot near the center of the target (Section 7). This system is represented in Figure 2.

Experiments were carried out to verify each element of the system. A successful demonstration shows the multi-layer control system achieving control of the active vehicle to keep it inside the error bounds while the laser endpoint is kept close to the center of the target. A 1 cm laser control tolerance was chosen to represent tight control that could be the hand-off to an even tighter optical metrology system. Future work will choose a tolerance that more closely represents the needs of a separated spacecraft interferometer.

5 GPS Position and Attitude Sensing

The primary goal of the coarse sensor for a formation of vehicles is to provide a global system that estimates relative position and attitude for all vehicles in the formation, within some tolerance. The demanded accuracy of the coarse sensor in this research is 2 cm. This accuracy is achieved through a GPS sensing system, utilizing differential carrier phase measurements. One vehicle collects the GPS phase data from both receivers, and processes it with an iterated extended Kalman filter (IEKF). Due to processor limitations, three vehicles are used for this arrangement. Two of the vehicles are under control, and the estimation process is performed on a third vehicle. The relative position and attitude estimates are then broadcast over the wireless ethernet to the other two vehicles for use in the control. The results show that the achieved position accuracies are well within 2 cm. Error in attitude estimates is indistinguishable from error in the overhead vision truth sensor.

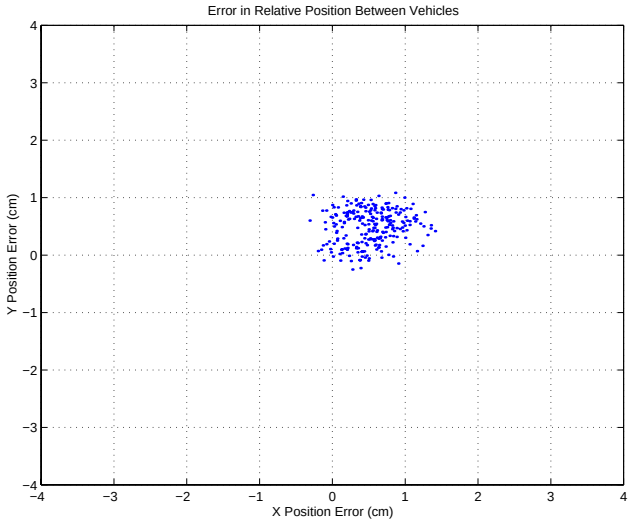

Figure 3: Error in the difference of the GPS and vision relative position solutions in X and Y for one pair of vehicles.

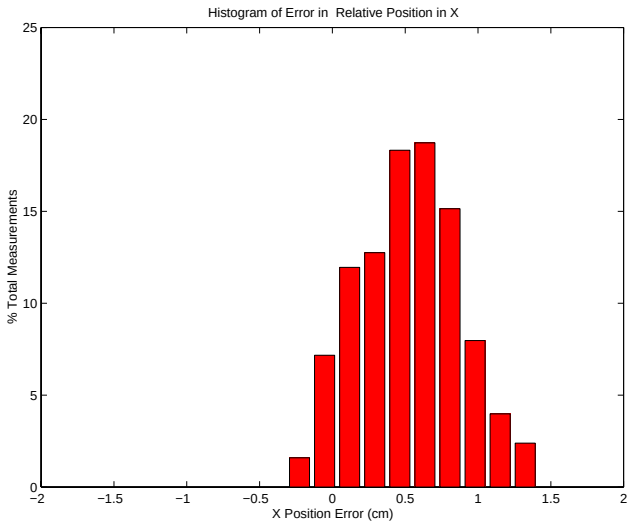

Figure 4: Distribution of the relative position errors, in the x direction.

Previous work with this GPS testbed has employed a weighted least squares algorithm [6, 9] for computing position and attitude estimates. Although this algorithm meets the 2 cm requirement for static tests, the performance of the estimator degrades when the vehicles move. Simula-

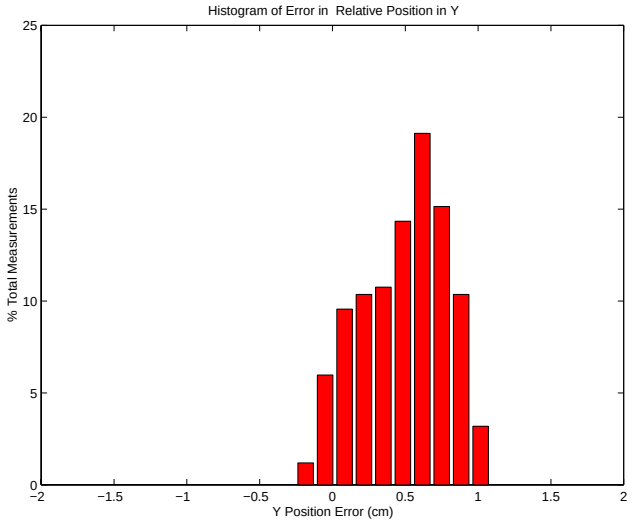

Figure 5: Distribution of the relative position errors, in the y direction.

tions with measured data suggested that using an IEKF algorithm would improve the accuracy of the position estimates [9] for both the stationary and dynamic cases. For this dynamic estimator, the vehicle velocity is estimated along with the position and attitude states.

A typical result for position error is shown in Figure 3. This data is for the case of one vehicle undergoing motion in a 360 cm^2 area over 30 seconds[1]. The mean of the error in radial distance is 0.78 cm, with a standard deviation of 0.32 cm. This error is well within the desired error bound. The distribution of errors is shown in Figure 4 and in Figure 5. Over 90 % of the errors in x and y are bounded by 1 cm. The results obtained with the IEKF algorithm are consistently better than those obtained with the weighted least squares algorithm, as described in Ref. [9].

Velocity states are estimated from changes in observed position, since no doppler measurements were made. As a result, some delay is apparent in these velocity estimates. Some delay is also introduced through the wireless ethernet. The control commands and the GPS measurements are both sent to the estimating vehicle, which then sends back the results of the estimation. The impact of this delay in the velocity estimates is described in the next section.

While the experimental errors are reported for a setup with the vehicles 1.2 m apart, the resultant accuracies easily extend to larger separations between vehicles. Since the sensor is measuring the phase of RF waves, errors will not scale with distance. The one noticeable dependence on distance is the magnitude of the effect of an attitude error. The attitude errors achieved in these experiments are within the error of the truth system. At larger distances, the baselines between the antennas can be increased to improve angular resolution if necessary.

[1]Previous experimentation has shown that this amount of motion is sufficient to cause large changes in the SNR values for each of the pseudolites.

6 Phase Plane Controller

A thruster control strategy was designed using phase plane techniques (see [14] for a discussion of nonlinear control systems). Spacecraft thruster position control systems (such as will be needed for NMI spacecraft) lend themselves to such techniques due to the nonlinear nature of the thrusters as well as the ability to create a simple M/s^2 model of the plant.

For the free-flying vehicles, control is implemented on each degree of freedom (two translation axes plus the orientation axis). The known characteristics of the system are used to generate families of possible trajectories in position-velocity space. There is a different family for each of three possible thrust conditions: positive, zero, or negative thrust; the magnitude of the thrust is considered constant. The trajectory that terminates at the origin is chosen as the desired trajectory and named the *switching line*. Then, the unit force (positive or negative) that moves the vehicle toward (or along) this trajectory is chosen. Once the vehicle reaches the origin, the thrusters are turned off until the state leaves the desired range, and the control process is repeated. The unit forces are mapped into vehicle thruster pairs.

The behavior near the origin is critical for the stationkeeping application. An *error bounding box* consisting of position and velocity error limits must be defined for each axis (x, y, and θ). When the vehicle state is outside the box, thruster firings are triggered as described above. When the state is moved back inside the box, the thrusters stay on until the velocity magnitude has decreased to less than a *deadband* which then causes the thrusters to turn off.

For each axis, the phase plane controller is thus defined by the parameters: position error bound, velocity error bound, velocity deadband, switching line curvature, and switching line offset. The deadband and offset parameters would be zero for the ideal case, but can be adjusted to reduce the effect of noise or lag in the sensor. The phase plane portrait in Figure 6 shows a typical layout of the bounding box and switching line for the control chosen for the active vehicle.

The parameters for control were initially chosen for the ideal case (deadband and offset set to zero). The switching line curvature is based on the acceleration from a thruster pair (i.e. $a = F/m$). This parameter was identified using a *prediction-error identification method* prior to running the control experiments. Curvature values were obtained for several thrust levels (which can be adjusted on the testbed vehicles by changing air pressure level). Within the multi-level controller, the objective of the coarse loop (GPS-based) is to keep the laser dot on the target. Thus the position and orientation error bounds were chosen so that the laser dot would be at the edge of the target just when the position and orientation are at the edges of their boxes. The rate error bounds were chosen to be larger than the sensor noise by roughly a factor of 3.

The effect of the sensing delays described in Section 5 is to

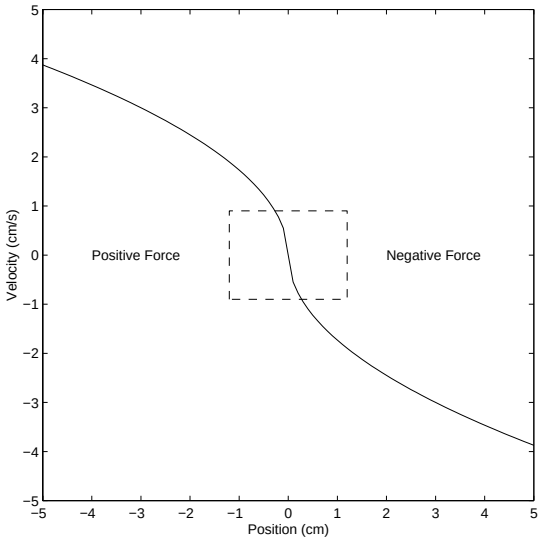

Figure 6: Phase plane portrait of controller.

Parameter	X	Y	Θ
position bound	1.2 cm	1.2 cm	0.05 rad
velocity bound	0.9 cm/s	0.9 cm/s	0.08 rad/s
deadband	0.6 cm/s	0.6 cm/s	0.02 rad/s
curvature	0.5 cm/s^2	0.5 cm/s^2	0.01 r/s^2
offset	1.2 cm	1.2 cm	0.05 rad

Table 1: The final parameters used in the phase plane controller

destabilize the system. Thus the control parameters were adjusted to increase system damping. This was achieved by adding the deadband and offset values. Also, the curvature of the switching line was reduced. These changes have the effect of damping the limit cycle created by the sensing delay. The final values used are shown in Table 1.

This controller was tested on the vehicle. The state estimate from the GPS/Kalman filter was the input and the output was thruster commands for the vehicle. A phase plane portrait containing 10 seconds of position and velocity data for movement in translation perpendicular to the path of the laser is shown in Figure 7. Notice that the velocity ranges from +2cm/s to −2cm/s. But the position is cycling around the negative position error bound of −1.2 cm. The position is inside the position bound 80 % of the time and never moves more than 6 mm beyond the bound. Similar performance is observed along the other translation axis and in orientation.

With disturbances and thruster modeling errors, we would not expect to bring the vehicle fully to rest. However, even with the delay inherent in the current sensing system (which will be improved in future work) it is quite promising that such tight control was nevertheless achieved.

The laser was tracked by the optical sensor as a metric (i.e. no feedback) during this test. The coarse controller keeps the laser on the target for most of the experiment, but the position of the dot moves randomly over the width of the target. This relatively poor targeting was expected because this coarse loop is designed only to bring the laser into

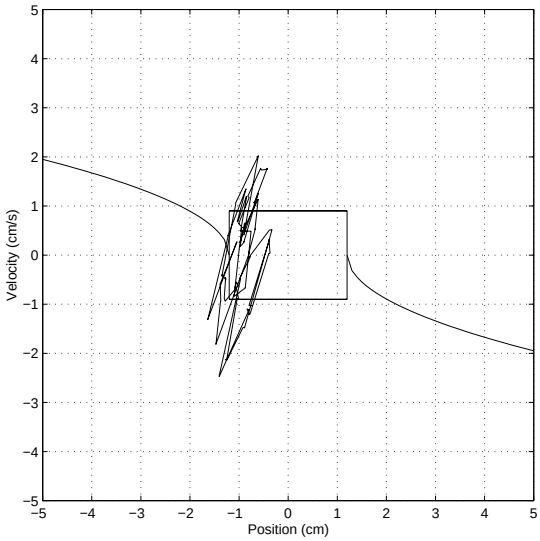

Figure 7: Phase plane portrait of controller performance.

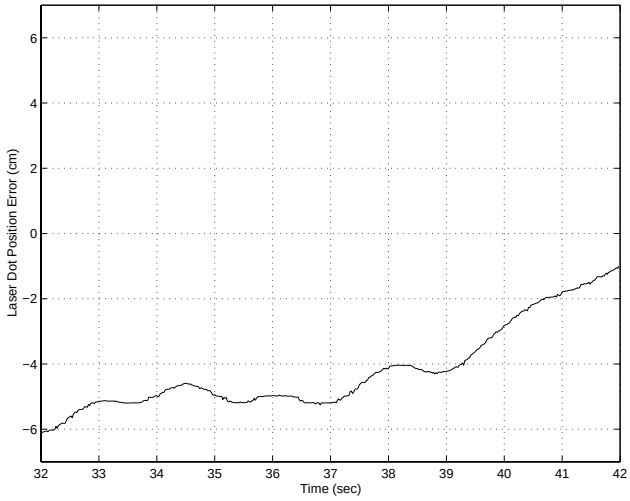

Figure 8: Laser tracking performance with only the coarse loop closed.

the field of view of the optical sensor. Figure 8 shows the distance of the laser from the center of the target during the same 10 seconds of data as shown in Figure 7. The optical control loop is closed on this sensor in the next section.

7 Optical Inner Loop

With the coarse GPS/thrusters control loop keeping the laser on target, the fine pointing optic/reaction wheel control loop was closed. For this initial test, these two control loops were designed and implemented separately. Future work will investigate the benefits of tighter coupling between the inner and coarse control loops. The wheel torques are expected to be small and can be treated as disturbances by the coarse loop. The optic sensor and reaction wheel are fast and accurate enough to detect motion due to the thruster control. This system is designed to demonstrate the validity of the control design, so a goal is set to significantly improve the pointing performance over the coarse loop alone; the laser dot was to be kept within 1 cm of the center of the target.

A simple proportional-derivative controller is used to generate torque commands based on the sensed laser end point

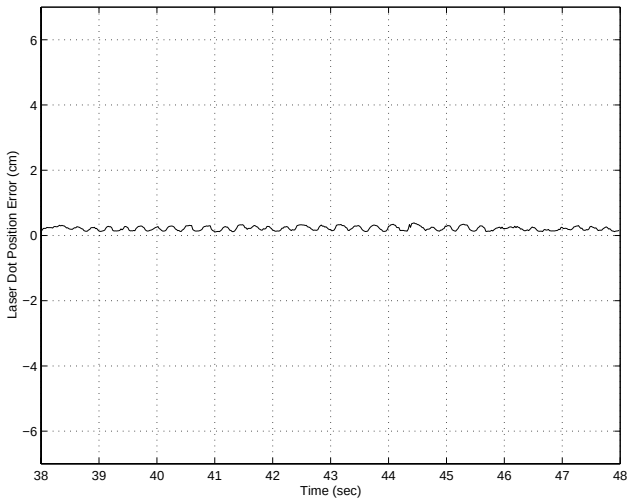

Figure 9: Laser tracking performance with both control loops closed.

position and velocity errors. When the laser point is not in view, the commanded torque is zero. The position gain was roughly twice the velocity gain.

A typical performance result with the fine pointing loop engaged is shown in Figure 9. Note the mean error is only 0.2 cm , and the deviation from zero is less than 0.4 cm. This corresponds to a significant improvement over the performance with only the coarse controller loop closed. The active vehicle's coarse loop control maintains vehicle position and orientation during this run.

8 Conclusions

This paper has demonstrated station keeping for a two-vehicle formation of spacecraft using GPS and a simple optical sensor. This problem has direct bearing on the separated spacecraft interferometer mission which needs precisely pointed yet widely separated optical instruments. A multi-layer control approach was successfully demonstrated for controlling the relative attitude and position of an active vehicle. It was shown that a coarse control loop using thrusters for actuation and GPS for relative sensing could keep station within specified error bounds. This in turn enabled a fine (but limited-range) optical sensor to be used for maintaining a more precise alignment of the vehicles.

The key technologies examined in this paper are: 1) the iterated extended Kalman filter applied to single- and double-difference GPS phase measurements that creates an accurate, but global sensor; 2) the use of a phase plane controller to enable thruster-based control with adjustable parameters that can be explicitly related to the alignment accuracy required to keep the laser on the target; and 3) the use of a multiple loop closure strategy for solving the difficult problem of very precise station keeping.

Future work will expand the control to 3 active vehicles. A new facility that is under development will allow much longer baselines between the vehicles ($\approx$ 10 m). These greater separations will also allow for a hardware test of the self-constellation concept. A more advanced laser metrology sensor will also be developed so that it can be replicated on each of the three vehicles. We will also investigate developing even tighter inner loops using fast steering mirrors.

References

[1] M. Colavita, K. Lau, and M. Shao, "The new millennium separted spacecraft interferometer," in *Space Technology and Applications International Forum*, (Albuquerque,NM), 1997.

[2] G. Purcell, D. Kuang, S. Lichten, S.-C. Wu, and L. Young, "Autonomous formation flyer (AFF) sensor technology development," in *AAS Guidance and Control Conference*, (Breckenridge,Colorado), Feb 1998.

[3] B. W. Parkinson and J. J. Spilker Jr., eds., *Global Positioning System: Theory and Applications*. Progress in Astronautics and Aeronautics, American Institue of Aeronautics and Astronautics, Inc., 1996.

[4] E. G. Lightsey, *Development and Flight Demonstration of a GPS Receiver for Space*. Dept. of Aeronautics and Astronautics, Stanford University, Stanford, CA, 94305, Jan. 1997.

[5] K. Lau, S. Lichten, L. Young, and B. Haines, "An innovative deep space application of GPS technology for formation flying spacecraft," in *Proceedings of the AIAA GNC Conf*, (San Diego, CA), July 1996.

[6] K. Zimmerman, *Experiments in the Use of the Global Positioning System for Space Vehicle Rendezvous*. Dept. of Aeronautics and Astronautics, Stanford University, Stanford, CA, 94305, Jan. 1996.

[7] S. Cobb, *Theory, Design, and Applications of GPS Pseudo-Satellites*. Dept. of Aeronautics and Astronautics, Stanford University, Stanford, CA, 94305, Aug. 1997.

[8] J. C. Adams, A. Robertson, K. Zimmerman, and J. P. How, "Technologies for spacecraft formation flying," in *Proceedings of the ION GPS-96 Conference*, (Kansas City, MO), Sept. 1996.

[9] T. Corazzini, A. Robertson, J. C. Adams, A. Hassibi, and J. P. How, "GPS sensing for spacecraft formation flying," in *Proceedings of the ION GPS-97 Conference*, (Kansas City, MO), Sept. 1997.

[10] K. R. Zimmerman and R. H. Cannon Jr., "Experimental demonstration of GPS for rendezvous between two prototype space vehicles," in *Proceedings of the ION GPS-95 Conf*, (Palm Springs, CA), September 1995.

[11] A. Conway, *Autonomous Control of an Unstable Model Helicopter Using Carrier Phase GPS Only*. Dept. of Aeronautics and Astronautics, Stanford University, Stanford, CA, 94305, Aug. 1995.

[12] D. T. Knight, "A new method for instantaneous ambiguity resolution," in *Proceedings of the Institute of Navigation 7th Int'l Tech. Mtg Conf*, (Salt Lake City, Utah), Sept. 1994.

[13] A. Hassibi and S. Boyd, "Integer parameter estimation in linear models with applications toGPS," in *Proceedings of 35th IEEE CDC*, (Kobe, Japan), Dec. 1996.

[14] D. Graham and D. McRuer, *Analysis of Nonlinear Control Systems*. John Wiley and Sons, Inc., 1961.